

# Influence of Calix[2]-*p*-benzo[4]pyrrole on the Electrochemical Properties of Poly(ethylene oxide)-Based Electrolytes for Lithium Batteries

A. Manuel Stephan,<sup>1</sup> T. Prem Kumar,<sup>1</sup> N. Angulakshmi,<sup>1</sup> P.S. Salini,<sup>2</sup> R. Sabarinathan,<sup>2</sup>  
A. Srinivasan,<sup>2</sup> Sabu Thomas<sup>3</sup>

<sup>1</sup>Electrochemical Power Systems Division, Central Electrochemical Research Institute, Karaikudi 630006, India

<sup>2</sup>Chemical Sciences and Technology Division, National Institute for Interdisciplinary Science and Technology, Thiruvananthapuram 695019, India

<sup>3</sup>School of Chemical Sciences, Mahatma Gandhi University, Kottayam 686560, Kerala, India

Received 11 June 2010; accepted 8 September 2010

DOI 10.1002/app.33462

Published online 10 December 2010 in Wiley Online Library (wileyonlinelibrary.com).

**ABSTRACT:** Poly(ethylene oxide) based electrolytes comprising LiCF<sub>3</sub>SO<sub>3</sub> and calix[2]-*p*-benzo[4]pyrrole (CBP) as anion binder were prepared and subjected to DSC, ionic conductivity, cationic transport number and FTIR analyses. Symmetric cells of the type Li/PEO+LiCF<sub>3</sub>SO<sub>3</sub>+CBP/Li were assembled with these electrolytes and evolution of interfacial resistance as a function of time was analyzed. The cationic transference number,  $t_{\text{Li}}^+$ , was found to increase from 0.23 to 0.78 on incorporation of CBP in the polymer electrolyte (PE). The incorporation of CBP as an anion trap does not enhance ionic conductivity

below 60°C although it improves the interfacial properties. FTIR study revealed the formation of Li–C compounds on the lithium surface upon contact with the CBP added membranes. The CBP added PE was found to be optimal in terms of ionic conductivity and transport number,  $t_{\text{Li}}^+$ , above 70°C, which were found to be higher for a system previously reported with calix[6]pyrrole. © 2010 Wiley Periodicals, Inc. *J Appl Polym Sci* 120: 2215–2221, 2011

**Key words:** lithium-polymer batteries; anion binder; ionic conductivity; transference number; interfacial properties

## INTRODUCTION

Although state-of-the art of lithium batteries are increasingly being used to power portable electronic devices such as laptop computers and cellular phones, the extension of their use in more demanding applications such as hybrid electric vehicles still requires optimization of crucial characteristics such as ionic conductivity and cationic transport number,  $t_{\text{Li}}^+$ .<sup>1</sup> Generally, nonaqueous lithium battery electrolytes are Lewis bases that interact with cations, which results in a high degree of ion pairing and in the formation of triplets and higher aggregates. Polarization losses in batteries are associated with low-ionic conductivity and lithium-ion transference number. In addition to the research on new salts and solvents, numerous attempts have been made to reduce ion association in nonaqueous electrolytes so as to enhance the transference number. Additives

capable of forming complexes not based on positively charged sites of hydrogen bonding find potential application in lithium batteries. For example, Lee et al.<sup>2,3</sup> introduced a new family of fluorinated boron compounds as anion receptors for nonaqueous liquid electrolytes. These electrolytes showed high-ionic conductivity and electrochemical stability.

Polymer electrolytes (PEs) possess several advantages over their liquid counterparts including such as absence of electrolyte leakage and internal shorting, and formation of noncombustible reaction products at the electrode surface.<sup>3–5</sup> Ionic dissociation in PEs is realized by use of lithium salts with low-lattice energy, addition of polar plasticizers and addition of complexing agents such as crown ethers or cryptands.<sup>6</sup> Extensive research has been made on poly(ethylene oxide) (PEO)-based electrolytes that have extremely strong solvating properties for a wide variety of salts through interaction of its ether oxygen with cations. Both anions and cations are mobile in PEs, with cationic transference numbers nearly always below 0.5. According to Golodnitsky et al.,<sup>7</sup> who studied the effect of calix[6]pyrrole on

Correspondence to: A. M. Stephan (arulmanuel@gmail.com).

the electrochemical properties of PEO-LiN(CF<sub>3</sub>SO<sub>2</sub>)<sub>2</sub>(LiTFSI) complexes, the anionic mobility reduces the limiting current density and forms an undesirable salt concentration gradient across the PE. Subsequently, this leads to a voltage drop during constant current operation, which in turn, affects the high-power capability of the battery. Also of importance is the fact that the mobile anions involve in unwanted electrode reactions and reduce the active area of the electrode.

Blazejczyk et al.<sup>8</sup> achieved a lithium-ion transport number equal to 1 with an appreciable conductivity and suggested that an anion-trapping mechanism was induced by the calixarene additive. Blazejczyk et al.<sup>9</sup> suggested use of less complex anion-binding receptors of more open conformation besides immobilization of anions and cations by interaction with their counterparts. This suggestion prompted us to initiate studies with calix[2]-*p*-benzo[4]pyrrole (CBP), a molecule that has a relatively open structure. Moreover, the presence of four NH units in CBP should, in principle, facilitate sufficient coordination. Although the lithium salts LiN(CF<sub>3</sub>SO<sub>2</sub>)<sub>2</sub> and LiN(C<sub>2</sub>F<sub>5</sub>SO<sub>2</sub>)<sub>2</sub> proved to be safe, thermally stable, and highly conducting, their application in lithium-ion batteries never materialized because it causes aluminum corrosion in electrolytes based on it.<sup>10</sup> On the other hand, lithium trifluoro methanesulfonate (LiCF<sub>3</sub>SO<sub>3</sub>) is highly resistant to oxidation, nontoxic, insensitive to ambient moisture when compared with LiPF<sub>6</sub> and LiBF<sub>4</sub>.<sup>11</sup> Hence, in the present study, we report the ionic conductivity and interfacial properties of PEO-based PEs incorporated with CBP and LiCF<sub>3</sub>SO<sub>3</sub>.

## EXPERIMENTAL PROCEDURE

### Synthesis of calix[2]-*p*-benzo[4]pyrrole

Calix[2]-*p*-benzo[4]pyrrole (p-6) containing two dipyrro-methane moieties and two *p*-phenylene units was synthesized as described earlier.<sup>12</sup> The bispyrrole intermediate, p-5, was first prepared as described in the literature.<sup>12,13</sup> The best yield of p-6 (77% isolated by crystallization from the crude reaction mixture with ethyl acetate/hexane) was obtained by treating a 0.006 M solution of p-5 in acetone/acetonitrile [1 : 12 (*v/v*)] with TFA (5 equiv). The macrocyclic structure of p-6 was confirmed by <sup>1</sup>H NMR, 2D-COSY, and FAB mass spectral analyses (see Figs. A1, A2, and A3 in Appendix).

### Preparation of PE membranes

PEO (*M<sub>w</sub>* = 200,000, Sigma-Aldrich) and LiCF<sub>3</sub>SO<sub>3</sub> (Sigma-Aldrich) were dried under vacuum for 2 days at 50°C and 60°C, respectively. Polymeric

**TABLE I**  
Composition of Polymer, CPB, LiCF<sub>3</sub>SO<sub>3</sub>, and *Q<sub>m</sub>* and *X<sub>c</sub>*

Samples	Composition	<i>Q<sub>m</sub></i> (J g <sup>-1</sup> )	<i>X<sub>c</sub></i> (%)	<i>t<sub>Li</sub></i> <sup>+</sup>
EO		218.3	64	
A	LiCF <sub>3</sub> SO <sub>3</sub> : (PEO) <sub>8</sub> : CBP <sub>0.25</sub>	127.2	58.2	0.23
B	LiCF <sub>3</sub> SO <sub>3</sub> : (PEO) <sub>8</sub> : CBP <sub>0.5</sub>	111.8	52.3	0.62
C	LiCF <sub>3</sub> SO <sub>3</sub> : (PEO) <sub>8</sub> : CBP <sub>1</sub>	102.2	46.8	0.78

membranes were prepared as follows. The composition of PEO, CBP, and LiCF<sub>3</sub>SO<sub>3</sub> are shown in Table I and are denoted as samples A, B, and C. To get a homogenous polymeric membrane, appropriate amounts of PEO, LiCF<sub>3</sub>SO<sub>3</sub>, and CBP were dissolved in tetrahydrofuran, stirred for 24 h and dried in vacuum for 12 h. The resulting mass was hot-pressed into films as described elsewhere.<sup>14,15</sup> The films had an average thickness of 30–50 μm. This procedure yielded homogenous and mechanically strong membranes, which were dried under vacuum at 50°C for 24 h for further characterization.

### Characterization of PEs

The ionic conductivity of the membranes, sandwiched between two stainless steel blocking electrodes (1-cm<sup>2</sup> diameter), was measured using an electrochemical impedance analyzer (IM6-Bio Analytical Systems) between a frequency range of 50 mHz and 100 kHz at various temperatures (0, 15, 30, 40, 50, 60, 70, and 80°C). Cells for compatibility studies were symmetric nonblocking cells of the type Li/PE/Li whose impedance under open-circuit conditions at 60°C was studied as a function of time. Values of *t<sub>Li</sub>*<sup>+</sup> were determined at 60°C for different contents of calixarene. The transference number of lithium ions as the carriers of charge flowing through the Li/PE/Li cell includes bulk and interfacial resistances, which can be calculated using the following equation

$$t_{\text{Li}}^+ = \frac{I_{\text{ss}}(V - I_0 R_0)}{I_0(V - I_{\text{ss}} R_{\text{ss}})} \quad (1)$$

where *R<sub>0</sub>* is the initial resistance of the SEIs (solid electrolyte interphase) formed at both the electrodes and *R<sub>ss</sub>* is the secondary passive-layer resistance. Differential scanning calorimetry and thermogravimetric measurements were performed at a rate of 10°C min<sup>-1</sup> in the temperature range 20–400°C.

The Li/PE interface was analyzed using FTIR (Thermo NICOLET Corporation, Nexus Model 670) by single internal reflection (SIR) mode.<sup>17</sup> The experimental set-up included a spectroelectrochemical cell in which the working electrode is a thin layer of gold (100 Å) deposited on a KBr window

using a special evaporation system (in high vacuum). The FTIR spectrometer operated in a glove box under H<sub>2</sub>O and CO<sub>2</sub>-free atmosphere, equipped with a grazing angle reflectance accessory (Spectratech) was used as described earlier.<sup>17</sup> The infra-red spectra were obtained at ambient temperature with an 8-cm<sup>-1</sup> resolution.

## RESULTS AND DISCUSSION

### DSC and TG analysis

Figure 1 shows the DSC profiles of PEO, and sample A, B, and C. A strong endothermic peak at about 65°C for PEO is attributed to eutectic and uncomplexed PEO.<sup>18</sup> Apparently, a shift occurs in the melting point on incorporation of LiCF<sub>3</sub>SO<sub>3</sub> (sample A). This shift moves further toward lower temperatures for CBP-containing samples (samples B and C) accompanied by a decrease in their heights, which indicates a reduction in the crystallinity of the sample. The degree of crystallinity,  $X_c$ , was calculated from the latent melting heat ( $Q_m$ ) for the PE and the latent melting heat of the crystalline PEO phase.

$$X_c = Q_m / Q_{mPEO} \quad (2)$$

In our study,  $Q_{mPEO}$  was found to be 218.3 J g<sup>-1</sup>. It can be seen from Table I that  $X_c$  decreases with the incorporation of calixarene. It is worthy to note that the introduction of LiCF<sub>3</sub>SO<sub>3</sub> into the polymer environment also reduces the crystallinity to some extent. The value of  $X_c$  calculated for the doped and undoped systems were normalized with respect to PEO. The apparent change in the values of  $X_c$  indicates interaction between CBP and lithium salt, lowering the degree of crystallinity.<sup>19</sup>

The TG and DTA traces of PEO, and samples A, B, and C are, respectively, depicted in Figure 2(a–d). A small endothermic peak can be observed below 50°C with a corresponding weight loss of ~ 2%, which is attributed to the removal of superficial moisture. Except at 66°C, no significant peak can be observed until 195°C at which irreversible decomposition starts. On the other hand, irreversible decomposition of the CBP-containing sample starts only at 250°C. This enhanced thermal stability of the CBP-containing electrolytes is presumably due to the higher decomposition temperature (above 300°C) of CBP (not shown here).

### Ionic conductivity and transference number

Arrhenius plots of CBP-free (PEO+LiCF<sub>3</sub>SO<sub>3</sub>) and CBP-added PEs are illustrated in Figure 3. It can be noted that ionic conductivity increases with increase in temperature for sample A. On addition of CBP in to the PEO matrix, ionic conductivity decreases up

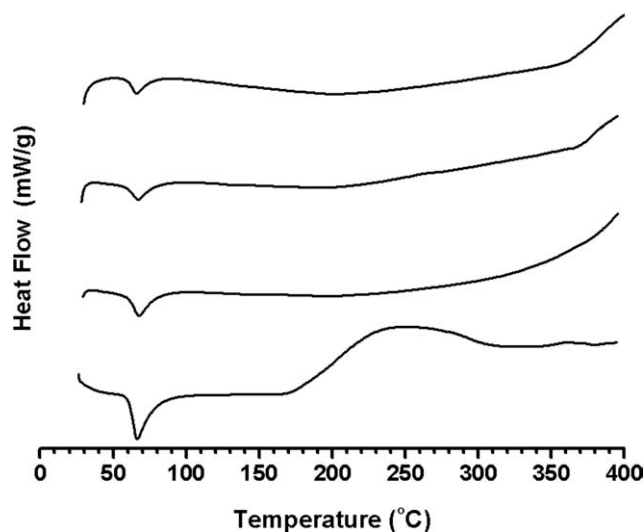


**Figure 1** DSC traces of PEO, sample (A) PEO+LiTF, (B) PEO+LiTF+5%CBP, and (C) PEO+LiTF+10%CBP.

to 50°C (sample B and C). However, above the melting point of crystalline PEO (60°C), ionic conductivity increased with an increase in the CBP content, as may be seen in the case of sample C. The exact mechanism by which ionic conductivity increases above the melting point of PEO due to addition of CBP is yet to be understood. However, the reduction in ionic conductivity on addition of CBP at temperatures below the melting point of PEO may be attributed to the “removal” of mobile charge carriers (anions) by CBP. According to Fuoss-Kraus calculations,<sup>20</sup> in the range where a rise in conductivity is noted, the contribution of free ions decreases due to generation of positively charged triplets.<sup>21</sup> According to Golodnitsky et al.,<sup>7</sup> this trend breaks down when such triplets aggregate into more complex species, making macroscopic viscosity the predominant factor in conductivity. Furthermore, bulky molecules in the electrolyte cannot only provide steric hindrance for segmental motion of the polyether chains but also render transport of ions more difficult. The present system exhibits higher ionic conductivity than those reported by Blazejczyk et al.<sup>9</sup> for the PEO- urea *p*-tert-butylcalix[4]arene incorporated complexes at 70°C.

In this study, both transference number and compatibility studies were made at 60°C because ionic conductivity at this temperature is found to be optimal for practical applications. It can be seen from the Table I that the value of  $t_{Li}^+$  for the PEO-LiCF<sub>3</sub>SO<sub>3</sub> system is 0.23, which lies in the normal range (0.2–0.3) for PEO-LiX systems.<sup>22,23</sup> The higher values of  $t_{Li}^+$  observed with electrolytes containing CBP may be attributed to preferential interaction of CBP with triflate anions rather than with lithium cations. The selective interaction enhances the ratio of cationic to anionic conductivity. Figure 4 illustrates a possible binding mode of anions with CBP. The results confirm

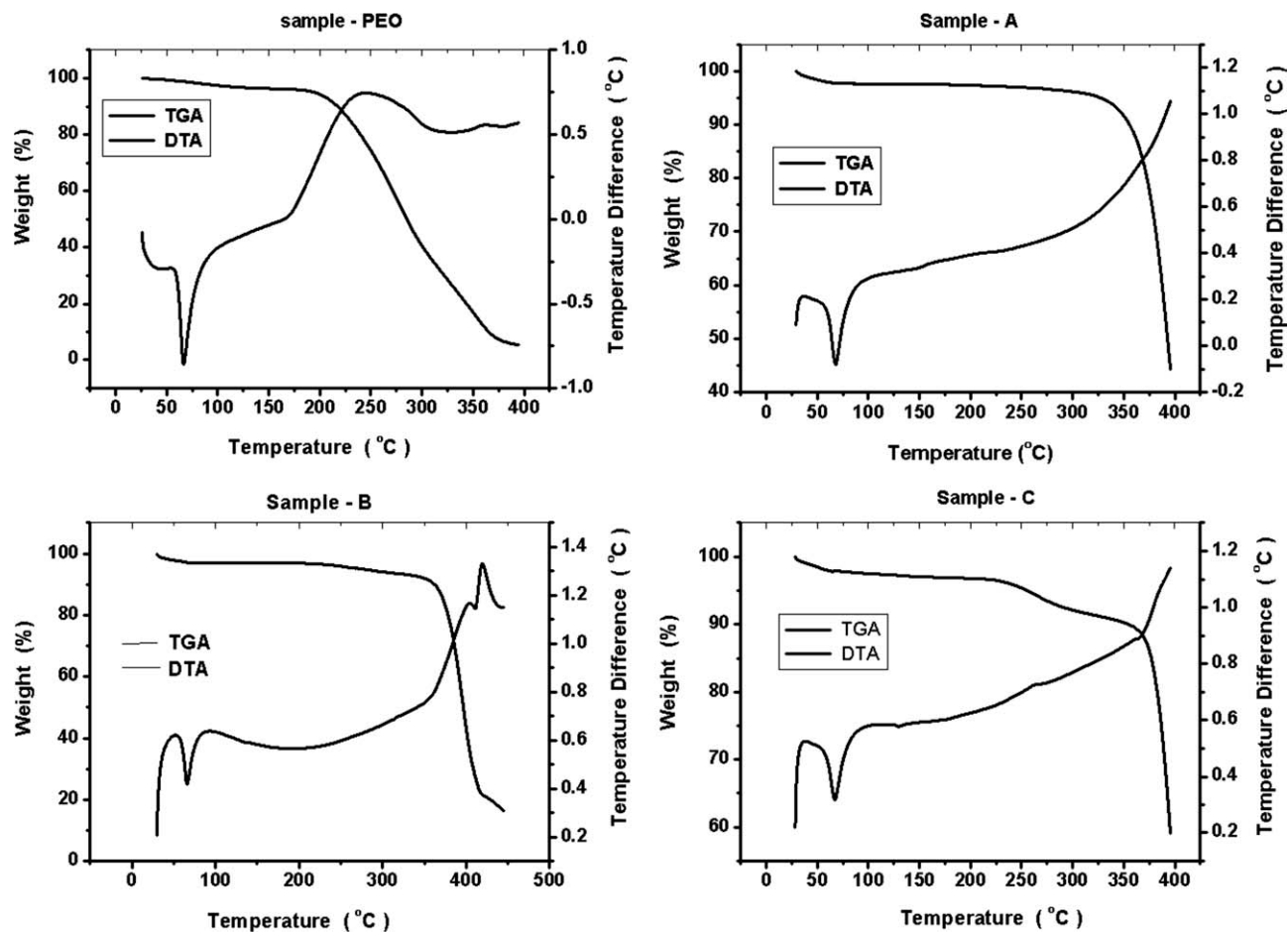


**Figure 2** TG-DTA traces of PEO, sample (A) PEO+LiCF<sub>3</sub>SO<sub>3</sub>, (B) PEO+LiCF<sub>3</sub>SO<sub>3</sub>+5% CBP, and (C) PEO+LiCF<sub>3</sub>SO<sub>3</sub>+10% CBP.

the expected role of CBP in forming stable complexes capable of diminishing the mobility of anions.

### Interfacial properties

The stability of the SEI originating from chemical impurities in the electrolyte or from salt precipitated

on the internal electrode surface can be measured by impedance spectroscopy. The transfer resistance of Li<sup>+</sup> ions generally depends on the type and concentration of the calixarene additive. Figure 5 displays the variation of the interfacial resistance as a function of time for Li/PEO+LiCF<sub>3</sub>SO<sub>3</sub>/Li and

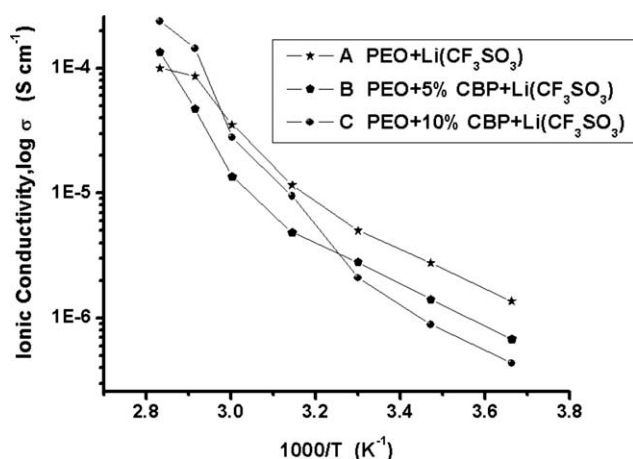


**Figure 3** Arrhenius behavior of PEO+Li(CF<sub>3</sub>SO<sub>3</sub>), PEO+5% CBP+Li(CF<sub>3</sub>SO<sub>3</sub>), and PEO+10% CBP+ Li(CF<sub>3</sub>SO<sub>3</sub>).

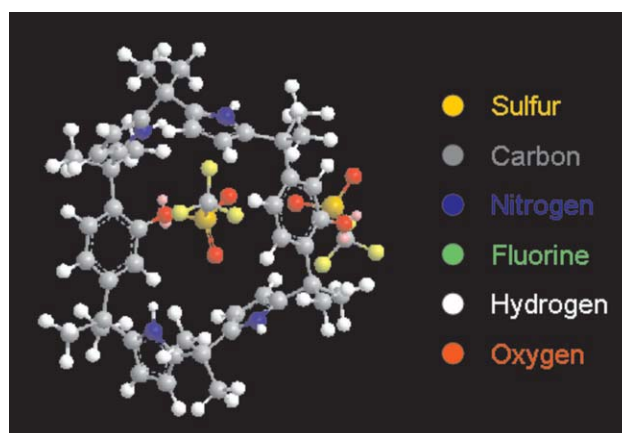


**Figure 4** The possible binding mode of anion with CBP. [Color figure can be viewed in the online issue, which is available at [wileyonlinelibrary.com](http://wileyonlinelibrary.com)]



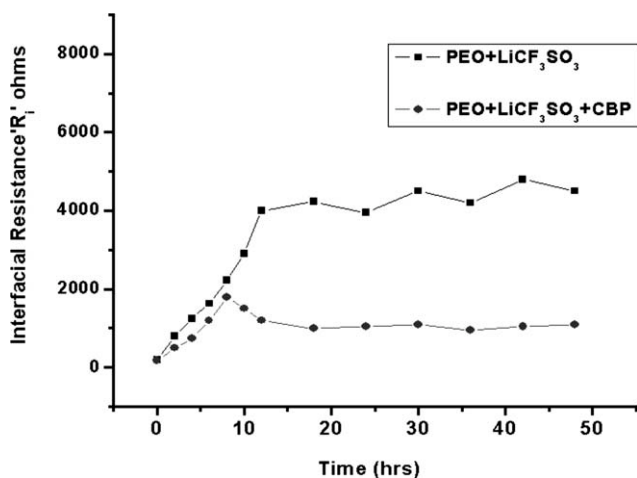


**Figure 5** Variation of interfacial resistance “ $R_i$ ” as a function of time for the symmetric cell comprising Li/PE/Li at 60°C.

Li/PEO+CBP+LiCF<sub>3</sub>SO<sub>3</sub> (sample C)/Li symmetric cell at 60°C. Our studies showed that sample C was optimal in terms of conductivity and of  $t_{Li}^+$ . The apparent reduction in the interfacial resistance of the calixarene-added sample is attributed to immobilization of anions by complexation, restricting their role in the formation of interfacial double layer on polarization of the cell. This may accelerate the growth of a secondary SEI layer through subsequent salt precipitation on the lithium electrode surface. Interfacial studies over longer duration would be justified if there is a sloping variation in the resistance with time. This is not just to suggest that the interfacial resistance will not vary at all over a period of days or month. However, any passive film formed on the initial SEI will in general be rather porous so as to allow penetration of the electrolyte into it. Thus, limiting this study to 50 h is justified.

According to Blazejczyk et al.,<sup>9</sup> supramolecules such as calixarenes in the PE environment promote the formation of strong hydrogen anion-receptor bonds in competition with anion-solvent, anion-cation, and other interactions. Furthermore, the receptors with low-protonic acidity<sup>24</sup> would contribute to passivation of the lithium electrode. In our study, CBP effectively purifies the electrolyte of associated and mobile anions, restricts the formation of passive layer in the polarized cell, and helps suppress growth of the SEI. This stable layer facilitates Li<sup>+</sup> charge transfer between the electrode and the electrolyte, a fact substantiated by the increase in the transference number.<sup>9</sup>

Figure 6(a–c) shows the FTIR spectrum of PEO+LiCF<sub>3</sub>SO<sub>3</sub>+CBP [a description of Fig. 6(a) is given below], Li after contact with PEO+LiCF<sub>3</sub>SO<sub>3</sub> [Fig. 6(b)], and PEO+LiCF<sub>3</sub>SO<sub>3</sub>+CBP [Fig. 6(c)] through KBr window at room temperature. The original features of the PE are absent in the spectra in Figure 6(b,c), but new peaks have arisen. In Figure 6(b), the bands between 3500 and 3800 cm<sup>-1</sup> are attributable to

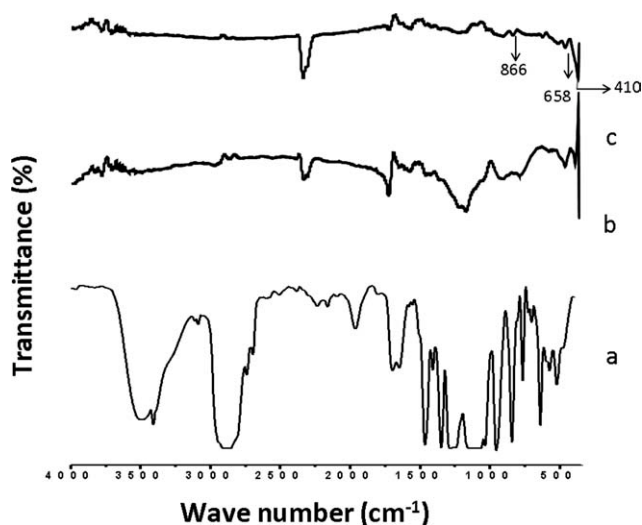


**Figure 6** FTIR spectra of (a) PEO+LiCF<sub>3</sub>SO<sub>3</sub>+10% CBP; lithium surface upon contact with (b) PEO+LiCF<sub>3</sub>SO<sub>3</sub> and (c) PEO+LiCF<sub>3</sub>SO<sub>3</sub>+10% CBP.

—OH group. The sharp peak at 1200 cm<sup>-1</sup> is attributed to the presence of —NH— group. New peaks emerge when lithium comes into contact with the CBP-containing electrolyte [Fig. 6(c)]. The peak at 866 cm<sup>-1</sup> arises due to formation of LiC<sub>2</sub>.<sup>24</sup> The broad band at 658 cm<sup>-1</sup> and the sharp peak at 410 cm<sup>-1</sup> indicate the formation of Li–C compounds<sup>17</sup> on the lithium surface on contact with CBP-containing membranes.

Shin et al.<sup>15</sup> report that commercially available PEO contains about 1 wt % of calcium compounds originating from the neutralization of the catalyst used in the synthesis. The CaO particles are very small and are intimately mixed with the PEO. PEO also contain up to 3 wt % of fumed silica, which is used to modify the fluidity of the polymer powder

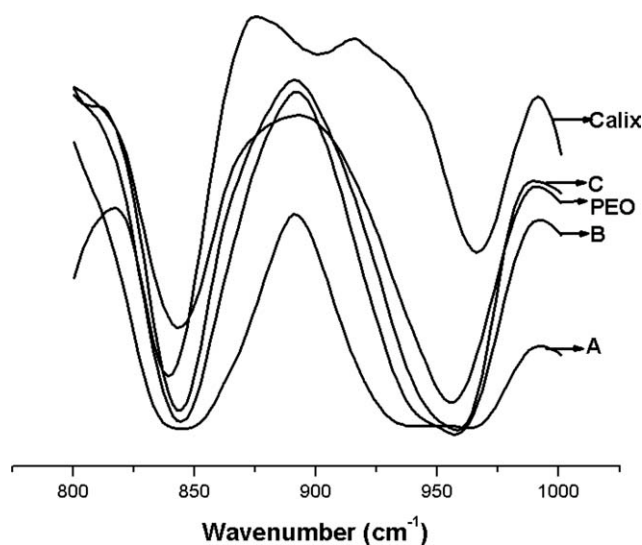


**Figure 7** FTIR spectrum of PEO, CBP, (A) PEO+LiCF<sub>3</sub>SO<sub>3</sub>, (B) PEO+LiCF<sub>3</sub>SO<sub>3</sub>+5%CBP and (C) PEO+LiCF<sub>3</sub>SO<sub>3</sub>+10%CBP.

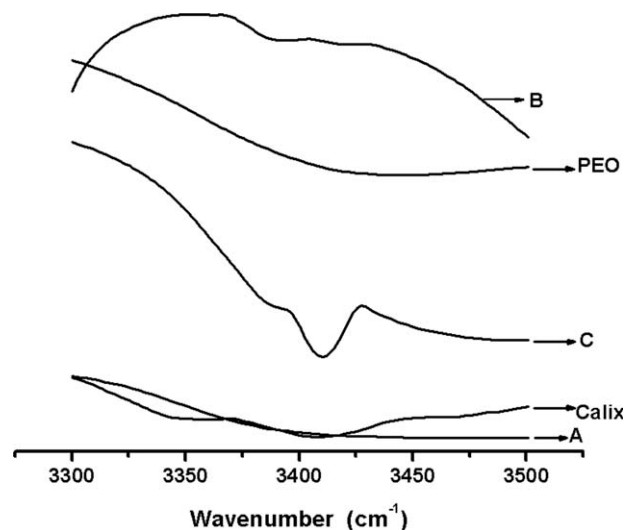


**Figure 8** FTIR spectrum of PEO, CBP, (A) PEO+LiCF<sub>3</sub>SO<sub>3</sub>, (B) PEO+LiCF<sub>3</sub>SO<sub>3</sub>+5%CBP and (C) PEO+LiCF<sub>3</sub>SO<sub>3</sub>+10%CBP.

during synthesis. Any one of these constituents may react with lithium and lead to the formation of new compounds (unassigned peaks) on the metal surface.

#### FTIR analysis

Figure 7 shows the spectrum of PEO, CBP, and samples A, B, and C. The spectral region 800–1000 cm<sup>-1</sup> depicts characteristic peaks of C–O stretching and –CH<sub>2</sub>– rocking modes.<sup>25</sup> A typical strong band with a maximum at 846 cm<sup>-1</sup> is assigned to the hybridized vibrations of the –CH<sub>2</sub>– rocking mode with a little skeletal C–O and C–C stretching motion mixed in. Similarly, the broad band that appears with maxima at 945 and 969 cm<sup>-1</sup> originates primarily from the C–O stretching motion with some contribution from the –CH<sub>2</sub>– rocking motion.<sup>25,26</sup> The broad shoulder that appears in PEO+LiCF<sub>3</sub>SO<sub>3</sub> complexes at 845 cm<sup>-1</sup> is assigned to the –CH<sub>2</sub>– rocking motion of complex formed between P(EO)<sub>3</sub> and LiCF<sub>3</sub>SO<sub>3</sub>.<sup>27</sup> It is interesting to note that no discernible peak has been identified in the high-energy narrow peak at 845 cm<sup>-1</sup> in the PEO+CBP+LiCF<sub>3</sub>SO<sub>3</sub> system, which suggests that the basic lithium–polyether backbone interactions remain unaltered.<sup>28</sup> A similar trend has been observed by Golodnitsky et al.,<sup>7</sup> who studied the electrochemical properties of calix[6]pyrrole.

The triflate anion, which is active in the IR region, has a broad band with a blurred maximum at 3500 cm<sup>-1</sup> (Fig. 8). On the other hand, a shoulder is developed ~3300 cm<sup>-1</sup> for the PEO+LiCF<sub>3</sub>SO<sub>3</sub> system. On incorporation of calix[2]-*p*-benzo[4]pyrrole in the PEO+LiCF<sub>3</sub>SO<sub>3</sub> system, the peak at 3405 is shifted to 3415 cm<sup>-1</sup>, which suggests local conformational changes in the CBP macromolecule arising from interactions of CBP with both LiCF<sub>3</sub>SO<sub>3</sub> and PEO, which is normally inactive in this vibration region.

## CONCLUSIONS

The effect of calix[2]-*p*-benzo[4]pyrrole (CBP) was prepared as an anion receptor in a PE was investigated for possible application in lithium batteries. The incorporation of CBP in a PEO environment considerably reduced the crystallinity of the polymer host. However, the ionic conductivity of electrolytes with CBP was found to be lower than that of a CBP-free electrolyte below the melting point of PEO. Above 60°C, the values of ionic conductivity of the samples were similar, irrespective of whether CBP was present or not. Although CBP does not play a significant role in the ionic conductivity, it improves the interfacial properties significantly. Interactions between the polymer host, CBP, and lithium salt are further inferred from FTIR results.

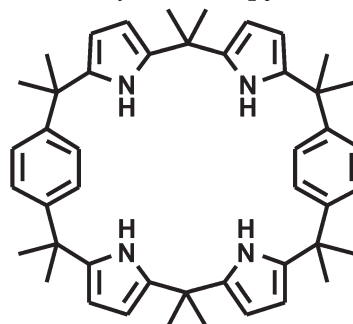
The Department of Science and Technology is gratefully acknowledged for financial support through SERC scheme.

## APPENDIX

### General information

NMR spectra were recorded with Bruker 500 MHz machine with CDCl<sub>3</sub> as solvent. Chemical shifts are expressed in parts per million (ppm) relative to TMS. FAB mass spectra were obtained on a JEOL SX-120/DA6000 spectrometer using argon (6 kV, 10 mA) as the FAB gas.

### Structure of calix[2]-*p*-benzo[4]pyrrole



### Spectral analysis of calix [2]-*p*-benzo[4]pyrrole (p-6)

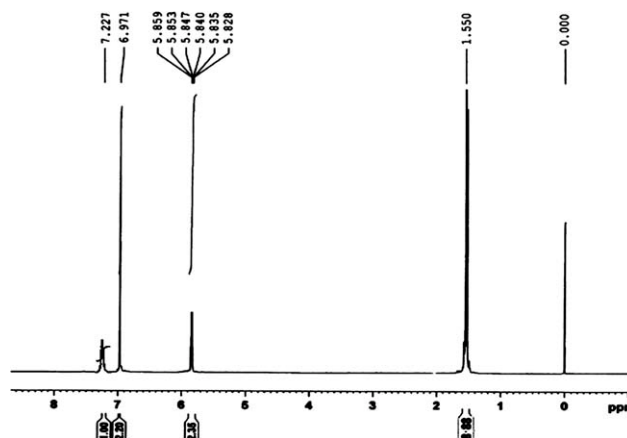


**Figure 1A** <sup>1</sup>H-NMR spectrum of p-6 in CDCl<sub>3</sub>.

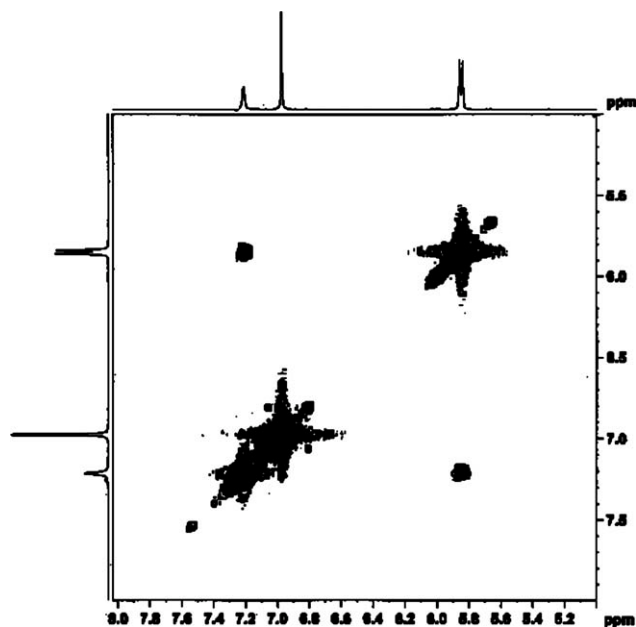


Figure 2A  $^1\text{H}$ - $^1\text{H}$  COSY spectrum of p-6 in  $\text{CDCl}_3$ .

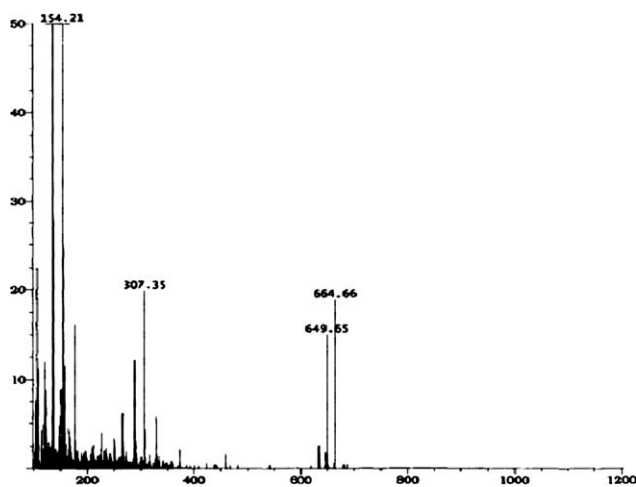


Figure 3A FAB MS Spectrum of p-6.

Exact mass: 664.45.

Molecular weight: 664.96

## References

1. Tarascon, J. M.; Armand, M. *Nature* 2001, 414, 359.
2. Lee, H. S.; Yang, X. Q.; Sun, X.; McBreen, J. C. *J Power Sources* 2001, 97-98, 566.
3. Lee, H. S.; Yang, X. Q.; McBreen, J.; Okamoto, Y.; Choi, L. S. *Electrochim Acta* 1995, 40, 2353.
4. Manuel Stephan, A. *Eur Polym J* 2006, 42, 21.
5. Manuel Stephan, A.; Nahm, K. S. *Polymer* 2006, 46, 5952.
6. McBreen, J.; Lee, H. S.; Yang, X. Q.; Sun, X. *J Power Sources* 2003, 89, 163.
7. Golodnitsky, D.; Kovarsky, R.; Mazor, H.; Rosenberg, Y.; Lapidés, I.; Peled, E.; Wieczorek, W.; Plewa, A.; Siekiński, M.; Kalita, M.; Settimi, L.; Scrosati, B.; Scanlon, L. *J Electrochem Soc* 2007, 154, A547.
8. Blazejczyk, A.; Wieczorek, W.; Kovarsky, R.; Golodnitsky, D.; Peled, E.; Scanlon, L. G.; Appetecchi, G. B.; Scrosati, B. *J Electrochem Soc* 2004, 151, A1762.
9. Blazejczyk, A.; Szczupzk, M.; Wieczorek, W.; Cmoch, P.; Appetecchi, G. B.; Scrosati, B.; Kovarsky, R.; Golodnitsky, D.; Peled, E. *Chem Mater* 2005, 17, 1535.
10. Krause, L. J.; Lamanna, W.; Summerfield, J.; Engle, M.; Kurba, G.; Loch, R.; Atanasaski, R. *J Power Sources* 1997, 68, 320.
11. Xu, K. *Chem Rev* 2004, 104, 4303.
12. Cafeo, G.; Kohnke, F. H.; White, A. P. J.; Garozzo, D.; Mesina, A. *Chem Eur J* 2007, 13, 649.
13. Sessler, J. L.; Cho, W. S.; Lynch, V.; Kral, V. *Chem Eur J* 2002, 8, 1134.
14. Manuel Stephan, A.; Prem Kumar, T.; Anbu Kulandainathan, M.; Angulakshmi, N. *J Phys Chem* 2009, 113, 1963.
15. Shin, J. H.; Alessandrini, F.; Passerini, S. *J Electrochem Soc* 2005, 152, A283.
16. Bruce, P. G.; Vincent, C. A. *J Electroanal Chem* 1987, 225, 1.
17. Chusid, O.; Gofer, Y.; Aurbach, D.; Watanabe, M.; Momma, T.; Osaka, T. *J Power Sources* 2001, 97-98, 632.
18. Robitaille, C. D.; Fauteux, D. *J Electrochem Soc* 1986, 133, 315.
19. Li, X.; Hsu, S. L. *J Polym Sci Polym Phys Ed* 1984, 22, 1331.
20. Fuoss, R.; Accascina, F. *Electrolytic Conductance*; Interscience: New York, 1959.
21. Zalewska, A.; Stygar, J.; Ciszewska, E.; Wittorko, M.; Wieczorek, M. *J Phys Chem B* 2001, 105, 5847.
22. Thomas, M. G. S. R.; Bruce, P. G.; Goodenough, J. B. *Solid State Ionics* 1985, 17, 5104.
23. Gray, F. M. *Polymer Electrolytes*; Royal Society of Chemistry: Cambridge, 1997.
24. Bondarenko, G. N.; Nalimova, V. A.; Fateev, O. V.; Guerard, D.; Semenenko, K. N. *Carbon* 1998, 36, 1107.
25. Bordwell, E.; Algrim, D. J.; Harrelson, J. *J Am Chem Soc* 1998, 110, 5903.
26. Lightfoot, P.; Mehta, M. A.; Bruce, P. G. *Science* 1993, 262, 883.
27. Papke, B. L.; Ratner, M. A.; Shriver, D. F. *J Phys Chem Solids* 1981, 42, 493.
28. Rhodes, C. P.; Fresh, R. *Solid State Ionics* 1999, 121, 91.